The Canadian Mineralogist
Vol. 45, pp. 457-469 (2007)
DOI: 10.2113/gscanmin.45.3.457

THE ATOMIC STRUCTURE AND HYDROGEN BONDING OF DEUTERATED MELANTERITE, $FeSO_4•7D_2O$

JENNIFER L. ANDERSON[§] AND RONALD C. PETERSON

Department of Geological Sciences and Geological Engineering, Queen's University, Kingston, Ontario K7L 3N6, Canada

IAN P. SWAINSON

Neutron Program for Materials Research, National Research Laboratory, Chalk River, Ontario K0J 1J0, Canada

ABSTRACT

The atomic structure of synthetic, deuterated melanterite ($FeSO_4•7D_2O$), *a* 14.0774(9), *b* 6.5039(4), *c* 11.0506(7) Å, β 105.604(1)°, space group $P2_1/c$, $Z = 4$, has been refined from the combined refinement of 2.3731(1) Å and 1.3308 Å neutron powder-diffraction data to a $Rwp_{(tot)} = 3.01\%$ and $Rp_{(tot)} = 2.18\%$. Both the short- and long-wavelength data were required to obtain a satisfactory fit in the Rietveld refinement. The results of this study confirm the previously proposed H-bonding scheme for melanterite. Small but significant variations of the Fe–O bond lengths are attributed to details of the hydrogen bonds to the oxygen atoms of the Fe octahedra. We draw comparisons between the monoclinic and orthorhombic heptahydrate sulfate minerals associated with mine wastes and relate differences in the structure to strengths and weaknesses in their H-bond networks.

Keywords: deuterated melanterite, hydrogen bonding, mine waste, sulfate minerals, crystal structure, neutron diffraction, epsomite.

SOMMAIRE

Nous avons affiné la structure cristalline de la mélanterite deutérée synthétique, ($FeSO_4•7D_2O$), *a* 14.0774(9), *b* 6.5039(4), *c* 11.0506(7) Å, β 105.604(1)°, groupe spatial $P2_1/c$, $Z = 4$, en utilisant une combinaison de données obtenues par diffraction de neutrons à 2.3731(1) Å et à 1.3308 Å, jusqu'à un résidu $Rwp_{(tot)}$ de 3.01% et $Rp_{(tot)}$ de 2.18%. Nous avons dû avoir recours aux données obtenues aux deux longueurs d'onde, courte et longue, afin d'obtenir un affinement convenable par la méthode de Rietveld. Nos résultats confirment le schéma de liaisons hydrogène proposé antérieurement pour la mélanterite. De légères mais importantes variations dans les longueurs des liaisons Fe–O sont attribuées aux détails des liaisons hydrogène avec les atomes d'oxygène des octaèdres Fe. Nous établissons des comparaisons entre les minéraux sulfatés heptahydratés de symétrie monoclinique et orthorhombique associés aux déchets miniers, et nous expliquons les différences structurales aux forces et faiblesses de leurs réseaux de liaisons hydrogène.

(Traduit par la Rédaction)

Mots-clés: mélanterite deutérée, liaisons hydrogène, déchets miniers, minéraux sulfatés, structure cristalline, diffraction de neutrons, epsomite.

INTRODUCTION

Melanterite ($FeSO_4•7H_2O$) is an oxidation-hydration by-product of sulfides. It commonly crystallizes from solution in areas where acid mine-waters become saturated in sulfate and Fe^{2+}. The melanterite structure is able to accommodate significant amounts of Cu, Zn (Peterson 2003a, Jambor 1994) and Mg (Peterson *et al*. 2006), and the degree of substitution is known to contribute to changes observed in the dehydration pathway of the mineral (Anderson & Peterson 2005). We present here the results of a structural investigation of deuterated melanterite.

DEHYDRATION PATHWAYS AND THE IMPORTANCE OF HYDROGEN BONDING

In the present study, we provide a detailed description of H-bonding in melanterite for comparison with the network of H-bonds in the group of orthorhombic heptahydrate sulfate minerals and products of dehydration with the general formula $M^{2+}SO_4•nH_2O$. The

§ *E-mail address*: anderson@geoladm.geol.queensu.ca

melanterite group comprises monoclinic heptahydrate minerals of the general formula $M^{2+}SO_4 \bullet 7H_2O$; M^{2+} = Fe, Cu, Co, Mg, Mn. A second group of heptahydrate minerals, the epsomite group [$M^{2+}SO_4 \bullet 7H_2O$; M^{2+} = Mg, Zn, Ni], has an orthorhombic structure. Although minerals of the epsomite and melanterite groups are not isostructural, many products of their dehydration are isostructural (Fig. 1). End-member melanterite dehydrates to the four-hydrate rozenite $FeSO_4 \bullet 4H_2O$, whereas Cu-substituted melanterite is known to dehydrate to siderotil $(Fe,Cu)SO_4 \bullet 5H_2O$ (Fig. 1) (Anderson *et al*. 2002, Jambor & Traill 1963, Peterson 2003b).

This investigation of the atomic structure and hydrogen bonding in melanterite complements earlier studies of the atomic structure (Baur 1967, Fronczek *et al*. 2001). Recently, the phase-stability behavior of melanterite and its dehydration products has been investigated by humidity-buffer methods (Anderson & Peterson 2005, Chou *et al*. 2002) and X-ray diffraction in a temperature- and relative-humidity-controlled environmental chamber (Peterson & Grant 2005).

Previous reports of the atomic structure of melanterite have included H-positions that were calculated (Baur 1967), or measured from single-crystal X-ray-diffraction data (Fronczek *et al*. 2001). In this study, the atomic structure and H-bonding of melanterite were refined in a combined refinement using long- and short-wavelength neutron-diffraction data. The data used in the following refinement were collected during a span of beam time granted to collect data for several hydrous sulfate minerals. Some of these minerals are dehydration products of melanterite- and epsomite-group minerals and, therefore, would not be suitable for single-crystal diffraction experiments.

Diffraction Experiments and Rietveld Refinement

Synthesis

Translucent green crystals of melanterite were synthesized at room temperature (22°C) in an air-tight glove box from a solution of reagent grade $FeSO_4 \bullet 7H_2O$ (Fisher I146) and 0.1 M D_2SO_4 (prepared from D_2O (AECL ZX098) and D_2SO_4 (C/D/N Isotopes Inc. D–39)). The reagent was dissolved completely in the dilute D_2SO_4 acid, and the solution was decanted into a shallow dish in a glove box. A strong desiccant (LiBr, Fisher L1117), was placed in the glove box to increase evaporation of the ferrous sulfate solution. The newly synthesized melanterite was redissolved in 0.1 M D_2SO_4, and the process repeated several times. The D:H ratio of a subsample of melanterite was measured qualitatively by infrared spectroscopy (IR) after each synthesis (Nicolet Avatar 320 Fourier–Transform IR with Golden Gate diamond-attenuated total internal reflection). Synthesis was repeated until the IR spectrum of melanterite showed a maximum D_2O:H_2O peak-height ratio. The final D:H ratio of the powder was measured by refinement of the occupancy factor of the proton sites (see Structure Refinement).

The synthesized crystals are euhedral, vitreous, 1–5 mm in diameter, and they display the crystal forms of a monoclinic prism and parallelohedron. Crystals intended for the neutron experiment were powdered, stored in a chamber of 69% relative humidity at 22°C, buffered by a saturated solution of KI in D_2O (Greenspan 1977). The sample was sealed in a vanadium sample can for the neutron-diffraction experiment with soft malleable indium wire to prevent dehydration or H – D exchange of the sample during data collection.

Diffraction experiments

Powder neutron-diffraction data for melanterite were collected at room temperature using the Dualspec C2 high-resolution constant-wavelength powder diffractometer of the NRU reactor at Chalk River Laboratories (Neutron Program for Materials Research (NPMR), Chalk River, Ontario, Canada). As a consequence of the space group and relatively large unit-cell volume of melanterite [974.5(1) $Å^3$], there is a large number of peaks in the diffraction dataset. The ability to resolve these peaks is compromised by the inherently broad peaks of the neutron-diffraction pattern. A neutron wavelength of 2.3731(1) Å was selected to minimize peak overlap and the broad line-shape that would result from the high density of melanterite peaks if a refinement were to be attempted with a shorter-wavelength neutron beam. This long-wavelength dataset was used in an accurate refinement of the unit-cell parameters of melanterite. The inclusion of a 1.3308 Å dataset with 1796 observations helps to compensate for the number of observations sacrificed by using a longer-than-normal wavelength of neutrons with only 738 observations. The combined refinement of the melanterite structure, using long- and short-wavelength data, resulted in the successful refinement of unit-cell parameters, atom positions, displacement parameters and site occupancies.

Powder neutron-diffraction data were collected over a scattering range of 20 to 100° 2θ. The wavelengths of

FIG. 1. Schematic diagram, with mineral names and formulae, showing the reversible hydration–dehydration phase changes that have been documented in M^{2+}–SO_4–H_2O systems. Documented phase-changes are indicated by double headed arrows, and only the two minerals at arrow heads are involved in the hydration–dehydration reaction. Pathways may differ with metal substitution, changes in acidity, relative humidity, temperature or sample history.

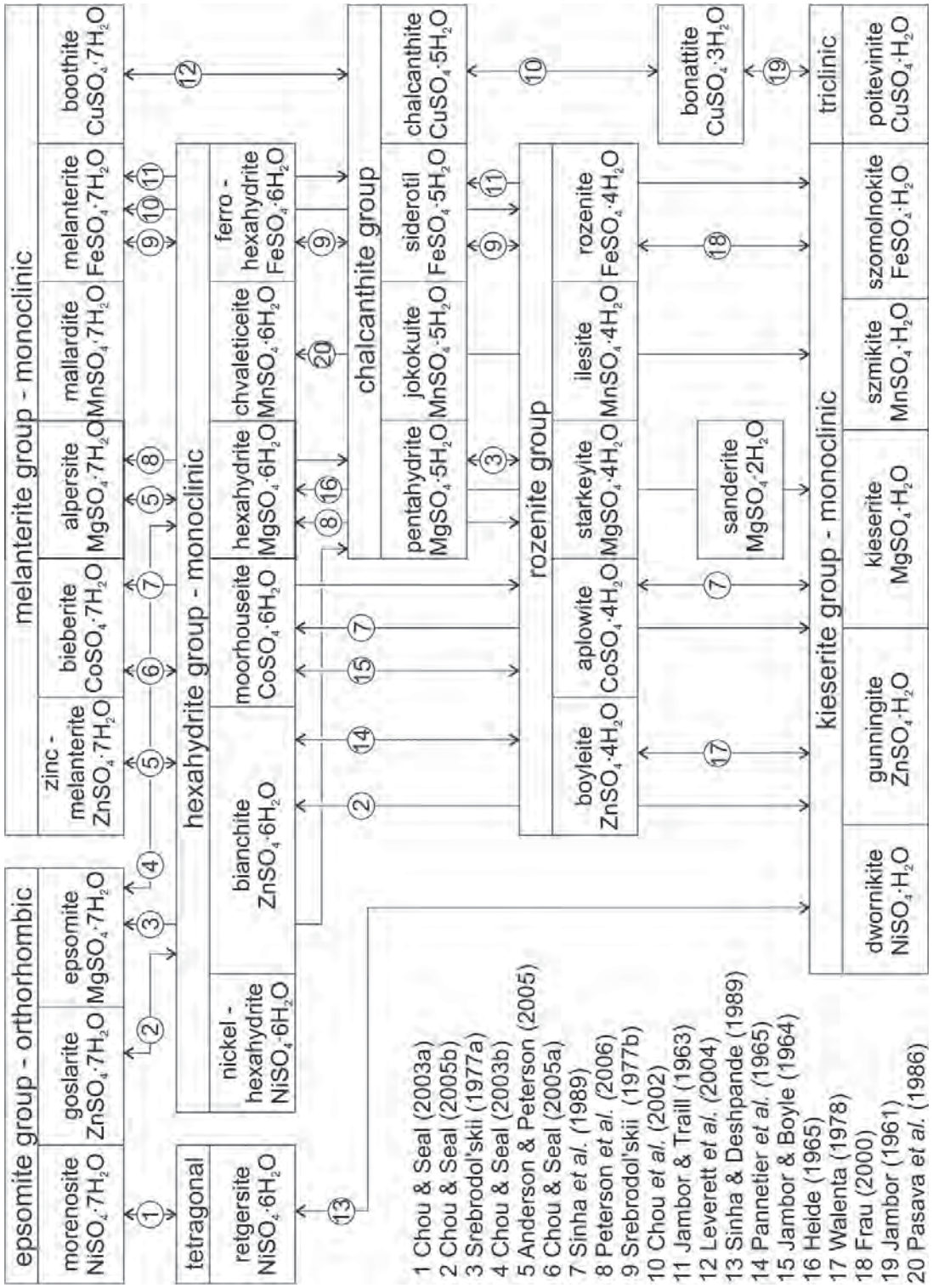
epsomite group - orthorhombic
morenosite NiSO4·7H2O
goslarite ZnSO4·7H2O
epsomite MgSO4·7H2O
melanterite group - monoclinic
zinc - melanterite ZnSO4·7H2O
bieberite CoSO4·7H2O
alpersite MgSO4·7H2O
mallardite MnSO4·7H2O
melanterite FeSO4·7H2O
boothite CuSO4·7H2O
tetragonal
retgersite NiSO4·6H2O
hexahydrite group - monoclinic
nickel - hexahydrite NiSO4·6H2O
bianchite ZnSO4·6H2O
moorhouseite CoSO4·6H2O
hexahydrite MgSO4·6H2O
chvaleticeite MnSO4·6H2O
ferro - hexahydrite FeSO4·6H2O
chalcanthite group
pentahydrite MgSO4·5H2O
jokokuite MnSO4·5H2O
siderotil FeSO4·5H2O
chalcanthite CuSO4·5H2O
rozenite group
boyleite ZnSO4·4H2O
aplowite CoSO4·4H2O
starkeyite MgSO4·4H2O
ilesite MnSO4·4H2O
rozenite FeSO4·4H2O
bonattite CuSO4·3H2O
sanderite MgSO4·2H2O
kieserite group - monoclinic
triclinic
dwornikite NiSO4·H2O
gunningite ZnSO4·H2O
kieserite MgSO4·H2O
szmikite MnSO4·H2O
szomolnokite FeSO4·H2O
poitevinite CuSO4·H2O
1 Chou & Seal (2003a)
2 Chou & Seal (2005b)
3 Srebrodol'skii (1977a)
4 Chou & Seal (2003b)
5 Anderson & Peterson (2005)
6 Chou & Seal (2005a)
7 Sinha et al. (1989)
8 Peterson et al. (2006)
9 Srebrodol'skii (1977b)
10 Chou et al. (2002)
11 Jambor & Traill (1963)
12 Leverett et al. (2004)
13 Sinha & Deshpande (1989)
14 Pannetier et al. (1965)
15 Jambor & Boyle (1964)
16 Heide (1965)
17 Walenta (1978)
18 Frau (2000)
19 Jambor (1961)
20 Pasava et al. (1986)

the neutron beam were calibrated in a separate experiment using the NIST standard Si 640c. The short- and long-wavelength datasets were collected over a period of 12 and 6 hours, respectively.

Refinement of the structure

The atomic structure of melanterite, including the D,H positions, were refined by least-squares refinement in a combined histogram Rietveld analysis of 2.3731(1) Å and 1.3308 Å wavelength powder neutron-diffraction data using the General Structure Analysis Software (GSAS) (Larson & Von Dreele 2000). The initial refinement of background and unit-cell parameters included only the 2.3731(1) Å diffraction data. The starting model was based on the atom coordinates and calculated H-positions determined by X-ray diffraction (Baur 1967). Peak shape, atom coordinates, isotropic displacement parameters and constrained site-occupancies for D sites were refined successfully, in that order, with the inclusion of the 1.3308 Å data. The D atom dominates the scattering and, ideally, the position of non-D atoms would be better resolved with single-crystal data or neutron-diffraction data on a non-deuterated specimen. To compensate for this, the S – O bond lengths of the sulfate tetrahedron were restrained to 1.47 ± 0.02 Å, based on the well-known geometry of the sulfate tetrahedron in sulfate minerals (Hawthorne *et al*. 2000). The final contribution of this restraint to the total chi-squared value of the refinement was 7.9% (Table 1).

In this refinement, we make two assumptions; first, each proton site is fully occupied with a mixture of D and H, and secondly, each site has the same D:H ratio, *i.e*., partitioning between crystallographically distinct proton sites does not occur. The site-occupancy values of each D site reflect the combined scattering-length of D and H at that site. Hydrogen, with a negative scattering length of –3.742(1) fm, will reduce the nuclear scattering of a site that is modeled to be fully occupied by D, with a scattering length of 6.674(6) fm. Given the coherent neutron-scattering lengths, the measured site-occupancy may be recalculated to obtain the D:H ratio of the proton sites (Table 2).

The final least-squares cycle yielded a final R_{wp} = 3.01%, R_p = 2.18% for the combined refinement (Table 1) and the observed and difference profiles are presented in Figure 2. The atom coordinates as determined by the combined refinement are presented in Table 2.

TABLE 1. CRYSTALLOGRAPHIC DATA AND REFINEMENT RESULTS FOR MELANTERITE BY THE COMBINED HISTOGRAM NEUTRON POWDER-DIFFRACTION REFINEMENT

Refinement results		Refinement statistics	
a (Å)	14.0774(9)	Neutron λ	2.3731(1) Å
b (Å)	6.5039(4)	# of observations	738
c (Å)	11.0506(7)	R*wp*	3.57%
β (°)	105.604(1)	R*p*	2.40%
V (Å^3)	974.5(1)		
		Neutron λ	1.3308 Å
		# of observations	1796
		R*wp*	2.63%
		R*p*	2.05%
		Total R*wp*	3.01%
		Total R*p*	2.18%
		Restraint contrib.	7.9%

$Rwp = \{\Sigma w(I_o - I_c)^2 / (\Sigma w I_o^2)\}^{1/2}$, $Rp = \Sigma(|I_o - I_c|) / \Sigma|I_o|$, restraint contribution = $[\chi^2_{(res)}/\#Obs_{(res)}] / [\chi^2_{(tot)}/\#Obs_{(tot)}]$. Space group: $P2_1/c$, $Z = 4$.

Discussion

Melanterite $FeSO_4 \bullet 7H_2O$, is monoclinic and crystallizes in the space group $P2_1/c$, with *a* 14.0774(9), *b* 6.5039(4), *c* 11.0506(7) Å, β 105.604(1)°, $Z = 4$. From the literature, we know that minerals of the melanterite group (M^{2+} = Co, Cu, Fe, Mg, Mn, Zn) consist of a sulfate tetrahedron, two crystallographically distinct M^{2+} atoms in octahedral coordination, with six H_2O groups forming the coordination sphere of each M^{2+} atom and one interstitial H_2O molecule that is not a direct ligand of an M^{2+} atom (Baur 1967, Fronczek *et al*. 2001). There are 14 unique H-bonds in the melanterite structure linking *M*1 octahedra to *M*2 octahedra

TABLE 2. ATOM COORDINATES, EQUIVALENT ISOTROPIC-DISPLACEMENT PARAMETERS AND D SITE-OCCUPANCY FACTORS FOR DEUTERATED MELANTERITE, ($FeSO_4 \bullet 7D_2O$)

	x	*y*	*z*	U_{iso}	Frac
Fe1	0	0	0	0.006(3)	
Fe2	0.5	0.5	0	0.005(3)	
S	0.2294(9)	0.475(2)	0.176(1)	0.007(6)	
O1	0.2076(9)	0.472(2)	0.038(1)	0.034(4)	
O2	0.1415(9)	0.537(2)	0.215(1)	0.015(4)	
O3	0.3109(9)	0.618(2)	0.229(1)	0.016(4)	
O4	0.2544(9)	0.266(2)	0.224(1)	0.026(5)	
Ow1	0.116(1)	0.388(3)	0.432(2)	0.053(7)	
Ow2	0.106(1)	0.954(3)	0.182(2)	0.034(5)	
Ow3	0.032(1)	0.787(2)	0.432(2)	0.030(6)	
Ow4	0.480(1)	0.454(3)	0.178(2)	0.036(6)	
Ow5	0.433(1)	0.283(3)	0.442(2)	0.038(6)	
Ow6	0.355(1)	0.855(2)	0.439(2)	0.030(5)	
Ow7	0.363(1)	0.002(3)	0.108(2)	0.037(5)	
D11	0.148(1)	0.262(2)	0.459(1)	0.039(6)	0.91(1)
D12	0.120(1)	0.428(3)	0.352(2)	0.050(6)	0.91(1)
D22	0.117(1)	0.816(2)	0.206(2)	0.041(6)	0.91(1)
D24	0.156(1)	0.050(3)	0.208(2)	0.044(5)	0.91(1)
D31	0.086(1)	0.874(2)	0.466(1)	0.017(4)	0.91(1)
D32	0.981(1)	0.882(2)	0.382(1)	0.038(5)	0.91(1)
D43	0.425(1)	0.520(2)	0.202(1)	0.033(5)	0.91(1)
D47	0.531(1)	0.464(2)	0.253(2)	0.051(6)	0.91(1)
D54	0.377(1)	0.286(2)	0.368(2)	0.040(6)	0.91(1)
D57	0.414(1)	0.369(3)	0.509(2)	0.065(7)	0.91(1)
D61	0.300(1)	0.919(2)	0.463(1)	0.033(5)	0.91(1)
D63	0.334(1)	0.774(2)	0.368(2)	0.050(5)	0.91(1)
D74	0.322(1)	0.080(3)	0.149(1)	0.042(6)	0.91(1)
D76	0.335(2)	0.884(3)	0.093(2)	0.096(9)	0.91(1)

The proton site is assumed to be fully occupied; a D site-occupancy factor of 0.91(1) is equivalent to a site occupancy of $D_{0.94}H_{0.06}$.

via the sulfate tetrahedra, creating a flexible undulating layer of repeating SO_4–*M*1–SO_4–*M*2 polyhedra (Fig. 3). The first five H-bonds link the *M*1 and SO_4 polyhedra within the layer in a pseudo-edge-sharing arrangement of bonds (Fig. 4). Likewise, the *M*2 and SO_4 polyhedra are linked within the layer by two H-bonds in a pseudo-edge-sharing arrangement and three H-bonds associated with the Ow7 H_2O molecule (Fig. 4). The remaining four H-bonds, of the 14 H-bonds in melanterite, bridge the layer of polyhedra and must break for the mineral to cleave along (001) (Fig. 3).

Previous work on the crystal structure of melanterite has shown that the *M*2 octahedron of the Fe^{2+} end-member deviates from ideal octahedral geometry (Baur 1967). This distortion from ideal octahedral geometry has been shown to increase with Cu-for-Fe substitution (Peterson 2003a). The distortion of octahedra is common among hydrated sulfates and is attributed to neighboring electrostatic effects communicated to the octahedra *via* H-bonds and where present, the square-planar distortion effects of Cu^{2+} (Strens 1966). The Fe–Ow bond lengths of octahedra in melanterite of this study range from

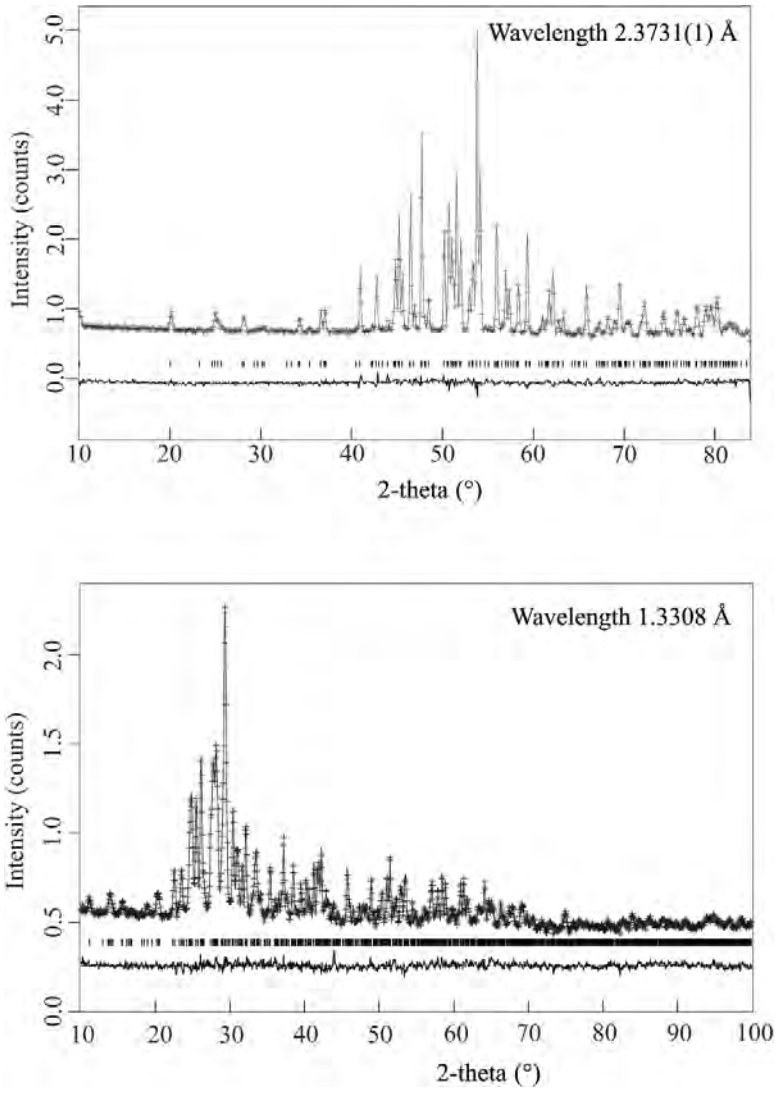

FIG. 2. Neutron-diffraction patterns of deuterated melanterite, λ = 1.3308 and 2.3731 Å. Observed data are shown as crosses, the fitted model as a straight line, and the difference (obs.–calc.) is displayed below.

2.08(2) to 2.19(2) Å, with a mean value of 2.12(2) Å (Table 3). The longest of these bonds is Fe2–Ow6 of the *M*2 octahedron [2.19(2) Å]. The Ow6 H_2O molecule is the only coordinated H_2O molecule in melanterite to receive an H-bond from a neighboring H_2O molecule. The Fe2–Ow6 bond lengthens to compensate for the increased bond-valence sum received by Ow6 as a result of the additional H-bond received from Ow7.

The H76 atom is equally likely to be H-bonded to Ow6 at 2.38(2) Å and O3 at 2.38(3) Å, as originally suggested by calculated and refined H-positions (Baur 1967, Fronczek *et al*. 2001). Although these H-bonds are the longest of the H-bonds in the structure, they are still within the range recognized in crystalline hydrates (<2.5 Å) (Ferraris & Franchini-Angela 1972, Fig. 5). Distances reported here plot significantly closer to the expected H–O and H...O values than the interatomic distances reported for the same bifurcated bond (Baur 1967, Fronczek *et al*. 2001, Kellersohn *et al*. 1991) (Fig. 5). The list of H-bonds presented in Table 3 includes all H–O distances less than 2.5 Å. The H-bond network of melanterite is represented schematically in Figure 6.

Hydrous sulfate minerals of the general formula $M^{2+}SO_4 \bullet nH_2O$ (n = 6, 7) can be divided into two groups: minerals with only one distinct octahedral *M* site and minerals with two distinct octahedral sites, each of which lies on an inversion center (Table 4, Fig. 7). Hydrous metal sulfate minerals with two distinct octahedral M^{2+} sites are observed to accommodate a wider range M^{2+} substitution than those containing only one crystallographically distinct *M* site. The ability to substitute metals of different radii and electronic configuration is enhanced with two distinct metal sites, each with different local environments.

Results of studies to test the extent of metal incorporation in $M^{2+}SO_4 \bullet nH_2O$ minerals corroborate the above statements. Goslarite, with one crystallographically distinct *M* site, is known to tolerate very limited substitution of Fe or Cu at 22°C (Anderson *et al*. 2005). Balarew & Karaivanova (1976) reported epsomite-group minerals to be stable in laboratory experiments at 25°C for crystal compositions of <3.20 wt.% $FeSO_4$ in goslarite $(Zn,Fe)SO_4 \bullet 7H_2O$, <0.05 wt.% $CuSO_4$ in Cu-substituted goslarite $(Zn,Cu)SO_4 \bullet 7H_2O$, and 2.30 wt.% Cu in Cu-substituted epsomite $(Mg,Cu)SO_4 \bullet 7H_2O$.

TABLE 3. SELECTED BOND-LENGTHS (Å) AND ANGLES (°) FOR MELANTERITE AS DETERMINED BY THE COMBINED HISTOGRAM NEUTRON POWDER-DIFFRACTION REFINEMENT

*M*1 octahedra		*M*2 octahedra		Sulfate tetrahedra	
Fe1-Ow1	2.10(2)	Fe2-Ow4	2.08(2)	S-O1	1.47(2)
Fe1-Ow2	2.17(2)	Fe2-Ow5	2.09(2)	S-O2	1.47(2)
Fe1-Ow3	2.10(2)	Fe2-Ow6	2.19(2)	S-O3	1.47(2)
				S-O4	1.47(2)
<Fe1-Ow>	2.12(2)	<Fe2-Ow>	2.12(2)		
				<S-O>	1.47(2)
Ow1-Fe1-Ow2	91.6(7)	Ow4-Fe2-Ow5	90.2(7)	O1-S-O2	110(1)
Ow1-Fe1-Ow2	88.4(7)	Ow4-Fe2-Ow5	89.8(7)	O1-S-O3	110(1)
Ow1-Fe1-Ow3	85.5(7)	Ow4-Fe2-Ow6	89.9(7)	O1-S-O4	109(1)
Ow1-Fe1-Ow3	94.5(7)	Ow4-Fe2-Ow6	90.1(7)	O2-S-O3	110(1)
Ow2-Fe1-Ow3	87.2(6)	Ow5-Fe2-Ow6	88.6(7)	O2-S-O4	107(1)
Ow2-Fe1-Ow3	92.8(6)	Ow5-Fe2-Ow6	91.4(7)	O3-S-O4	111(1)
<Ow-Fe1-Ow>	90.0(1)	<Ow-Fe2-Ow>	90.0(1)	<O-S-O>	109(1)

D_2O molecule	*O*···D	D-Ow	Ow-D	D···*O*	D-D	D-O-D
O1···D11-Ow1-D12···*O2*	1.84(2)	0.94(2)	0.94(2)	1.76(2)	1.58(2)	113(3)
O2···D22-Ow2-D24···*O4*	1.85(2)	0.94(2)	0.93(2)	1.95(2)	1.62(2)	120(3)
O1···D31-Ow3-D32···*O2*	1.95(2)	0.95(2)	0.99(2)	2.04(2)	1.52(2)	103(2)
O3···D43-Ow4-D47···*Ow7*	1.84(2)	0.98(2)	0.94(2)	1.84(2)	1.49(2)	102(2)
O4···D54-Ow5-D57···*Ow7*	2.01(2)	0.97(2)	1.01(2)	1.68(2)	1.60(2)	108(2)
O1···D61-Ow6-D63···*O3*	1.86(2)	0.97(2)	0.92(2)	1.79(2)	1.58(2)	112(2)
O4···D74-Ow7-D76···*Ow6*	1.86(2)	0.97(2)	0.86(2)	2.38(2)	1.45(2)	104(3)
O4···D74-Ow7-D76···*O3*				2.38(3)		
<*O*···D-Ow-D···*O*>			0.95(2)	1.94(2)	1.55(2)	109(2)

Descriptions of natural occurrences of the $NiSO_4•6H_2O$ minerals indicate that nickelhexahydrite, with two crystallographically unique *M* sites, is able to tolerate more metal-substitution than retgersite, with only one crystallographically unique *M* site. Oleinikov *et al*. (1965) and Eliseev & Smirnova (1958) reported MgO + FeO + CuO values of 12.42, 5.32 and 6.4 wt.% in nickelhexahydrite crystals. No significant metal-substitution has been reported in retgersite.

Minerals of the melanterite group, having two crystallographically distinct *M* sites, are stable at 25°C with crystal compositions >34 mol.% Fe in the Zn–Fe system, <42 mol.% Cu in the Zn–Cu system, and >49 mol.% but <55 mol.% Cu in the Mg–Cu system at 25°C (Balarew & Karaivanova 1976). The name *alpersite* was recently approved for Mg-dominant minerals with the melanterite structure, the type specimen containing 58 mol.% Mg (Peterson *et al*. 2006). Little is known about site-specific substitution of metals in the hexahydrite group of minerals; however, the network of H-bonds surrounding the M^{2+} octahedra in the structure of the hexahydrite group shares some similarities with that of the melanterite-group structure. Both the melanterite- and hexahydrite-group structures contain two unique octahedral *M* sites, one accepting an additional H-bond and one that is ideal in that it donates 12 H-bonds and received no additional H-bonds.

Despite their differences, the monoclinic and orthorhombic heptahydrate structures share many physical properties. The heptahydrate minerals are easily dissolved in water, readily hydrated or dehydrated during small changes in temperature and relative humidity, and both have a perfect cleavage. The cleavage plane in both structures is parallel to the layer composed of M^{2+} octahedra linked *via* H-bonds to SO_4 tetrahedra. This layer topology is present in melanterite parallel to (001) and in epsomite parallel to (010). The layer structures of the heptahydrate minerals are illustrated in Figures 4 and 8. In both structures, there are four unique H-bonds per formula unit (16 H-bonds per unit cell) that must be broken for the mineral to cleave along this surface.

A closer look at the H-bond network within these layers and a comparison of the crystal structures of the monoclinic and orthorhombic heptahydrate minerals reveal an explanation for the differences in the ability of the two minerals structures to tolerate M^{2+} substitution.

The topology of the layer structures of melanterite- and epsomite-group minerals is similar in that each structure has 14 unique H-bonds. In both structures, there are 10 H-bonds within the layer structure and four H-bonds that bridge the layer and must be broken for the mineral to cleave. The interstitial H_2O molecule is held within the layer of both structures by three H-bonds, with the fourth H-bond associated with the interstitial H_2O molecule bridging the layer. The seven remaining H-bonds within the layer structures link the M^{2+} and SO_4 polyhedra to each other. In epsomite, six of these seven H-bonds are arranged between the M^{2+} octahedron and SO_4 tetrahedra in a pseudo-edge-sharing arrangement. In the layer structure of melanterite, the three H-bonds associated with Ow7 and bonded within the layer form a linkage between one *M*2 site and the next and do not interact with the *M*1 site. The only other H-bonds associated with the *M*2 site are the two in a pseudo-edge-sharing arrangement between *M*2 and SO_4. The five remaining H-bonds, of the seven that link polyhedra within the melanterite layer, link the *M*1 octahedra to the SO_4 tetrahedra *via* pseudo-face- and edge-sharing polyhedra.

Whereas both structures are H-bonded across the layer structure by four H-bonds, the *M* site in epsomite-group minerals is associated with three of these H-bonds and the fourth, as previously mentioned, is associated with the interstitial H_2O molecule. In melanterite-group minerals, the *M*1 site contributes one of the four H-bonds that bridge the layer, the *M*2 site contributes two and the Ow7 contributes the last.

These differences between the two heptahydrate structures provide an explanation for differences in the wavelengths of the layers and the increased flexibility in the melanterite structure. This flexibility allows the mineral to accommodate an M^{2+} polyhedron occupied by different ions. The more compact linkage of H-bonds in epsomite-group minerals restricts the substitution of metals.

Summary

Melanterite is commonly the most abundant mineral in acid mine-waste systems and is known to accommodate significant amounts of M^{2+} substitution (Jambor 1994). The ability of the melanterite structure to tolerate

TABLE 4. SUMMARY OF MINERAL GROUPS WITH THE GENERAL FORMULA ($M^{2+}SO_4•nH_2O$, n = 6, 7) CONTAINING 1 OR 2 CRYSTALLOGRAPHICALLY DISTINCT M SITES IN OCTAHEDRAL COORDINATION WITH 6 H_2O GROUPS

One *M* site	Two *M* sites
Epsomite group $P2_12_12_1$	Melanterite group $P2_1/c$
goslarite $ZnSO_4•7H_2O$	alpersite $(Mg,Cu)SO_4•7H_2O$
epsomite $MgSO_4•7H_2O$	bieberite $CoSO_4•7H_2O$
morenosite $NiSO_4•7H_2O$	boothite $CuSO_4•7H_2O$
	mallardite $MnSO_4•7H_2O$
	melanterite $FeSO_4•7H_2O$
	zinc-melanterite $(Zn,Cu,Fe)SO_4•7H_2O$
Retgersite $P4_12_12_1$	Hexahydrite group $C2/c$
retgersite $NiSO_4•6H_2O$	bianchite $(Zn,Fe)SO_4•6H_2O$
	chvaleticeite $(Mn,Mg)SO_4•6H_2O$
	ferrohexahydrite $FeSO_4•6H_2O$
	hexahydrite $MgSO_4•6H_2O$
	moorhouseite $(Co,Ni,Mn)SO_4•6H_2O$
	nickelhexahydrite $(Ni,Mg,Fe)SO_4•6H_2O$

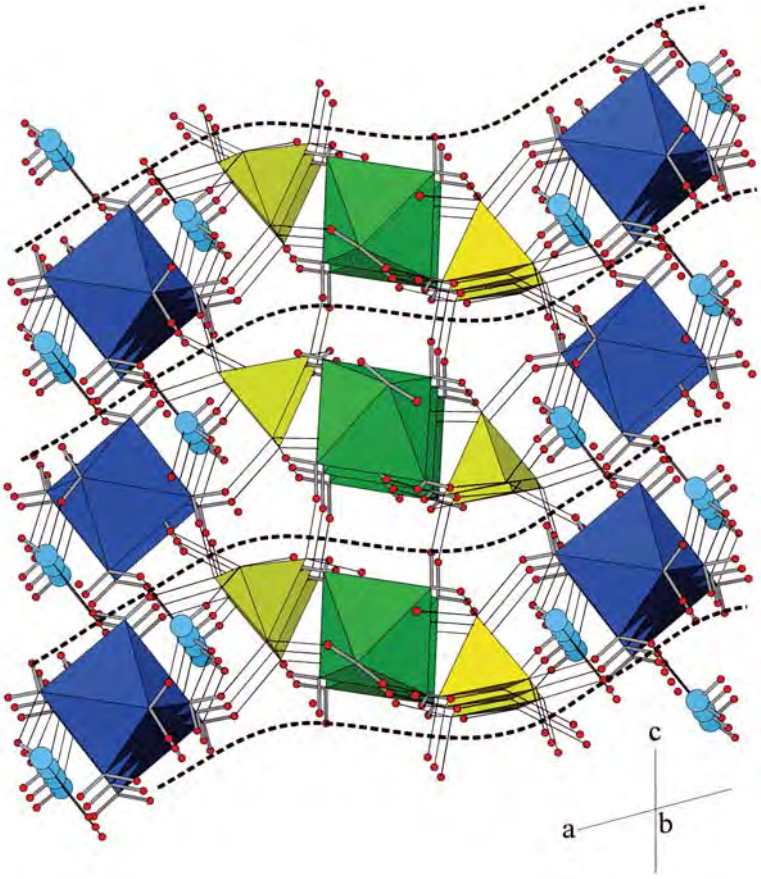

FIG. 3. Schematic representation of the atomic structure of melanterite (ATOMS 6.0, Dowty 1995). The undulating layer-structure parallel to the (001) perfect cleavage is illustrated here and is indicated by the dashed black line. Chains of *M*1 octahedra (green) are linked to chains of *M*2 octahedra (blue) *via* H-bonds to chains of sulfate tetrahedra (yellow), creating a layer of repeating chains of SO_4–*M*1–SO_4–*M*2 polyhedra. The interstitial H_2O molecule is H-bonded between the *M*2 octahedra and the SO_4 tetrahedra in the melanterite structure. The layer structure is bridged by four unique H-bonds per formula unit.

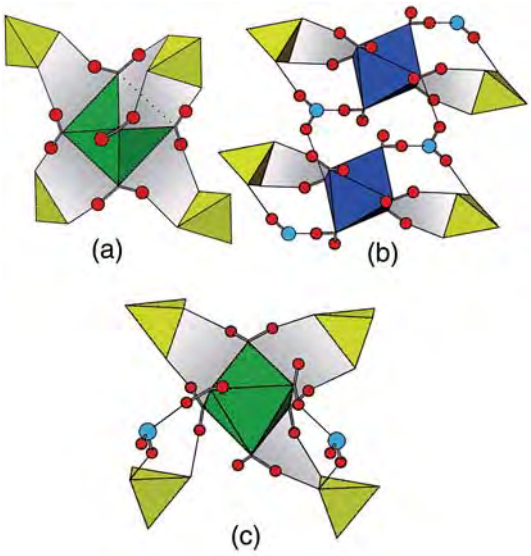

FIG. 4. Details of the *M*–SO_4–*M* polyhedron linkages within the layer structure of minerals in the melanterite and epsomite groups (ATOMS 6.0). (a) The *M*1 octahedra in melanterite-group minerals are linked to the SO_4 tetrahedra in a pseudo-edge- and face-sharing arrangement of H-bonds. (b) The *M*2 and SO_4 polyhedra in melanterite-group minerals are linked *via* the interstitial H_2O molecule and a pseudo-edge-sharing arrangement of H-bonds. (c) In epsomite-group minerals, six of the seven H-bonds within the layer structure are linked in a pseudo-edge-sharing arrangement between the M^{2+} octahedra and SO_4 tetrahedra.

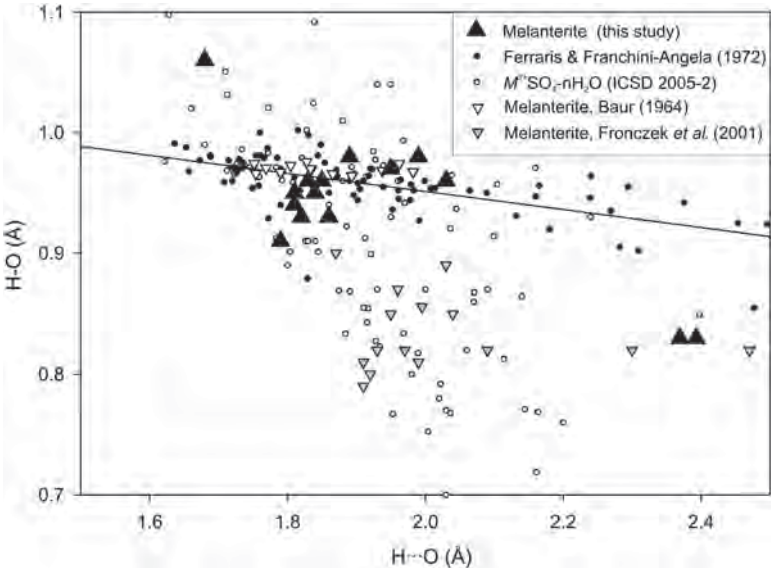

FIG. 5. Plot of H–O and H-bond distances in the H_2O molecule. Small closed circles and line of least-squares fit represent data from Ferraris & Franchini-Angela (1972). Small open circles represent data from the following papers: Angel & Finger (1988), Bacon & Titterton (1975), Bargouth & Will (1981), Baur (1962, 1964a, b, 1967), Baur & Rolin (1972), Blake *et al*. (2001), Calleri *et al*. (1984), Elerman (1988), Gerkin & Reppart (1988), Hawthorne *et al*. (1987), Held & Bohaty (2002), Iskhakova *et al*. (1991), Kellersohn (1992), Kellersohn *et al*. (1991), Ptasiewicz-Bak *et al*. (1993), Wildner & Giester (1991), Zahrobsky & Baur (1968), Zalkin *et al*. (1967). The solid circles and linear-regression line represent the birfurcated and non-bifurcated H-bonds from the survey of neutron-diffraction studies (Ferraris & Franchini-Angela 1972). Hydrogen bonds determined by X-ray diffraction are significantly shorter than those determined by neutron diffraction.

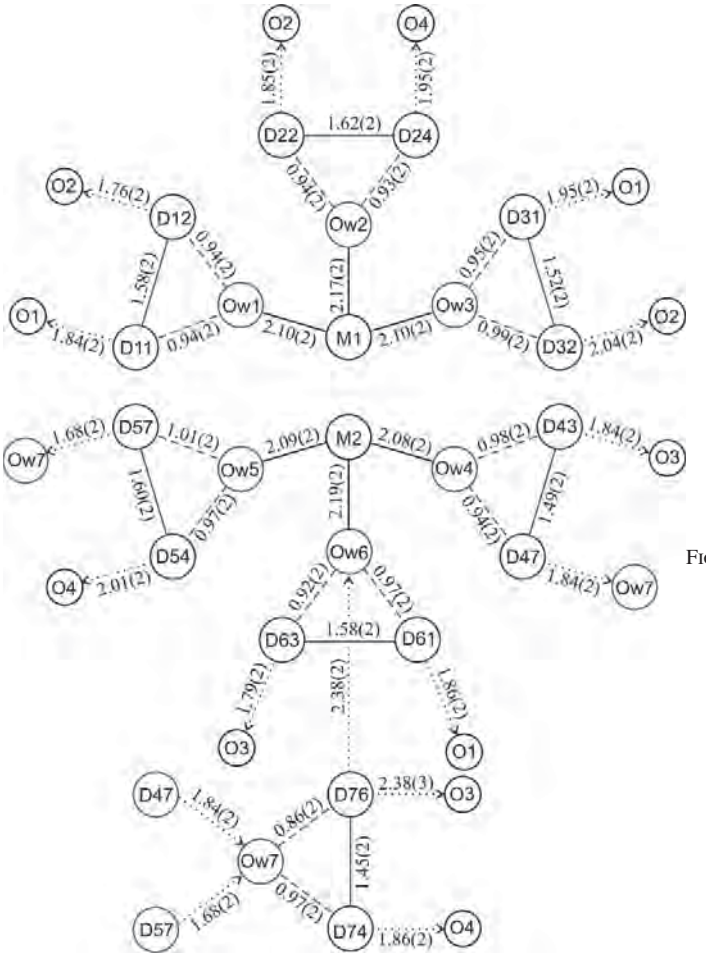

FIG. 6. Schematic diagram of the network of H-bonds in melanterite, as determined by the combined-histogram powder neutron-diffraction refinement of deuterated melanterite, $FeSO_4 \cdot 7D_2O$. The O–H distances (Å) are indicated by the dashed lines. Dotted lines represent H-acceptor bonds. This diagram is not to scale, and only represents the topology of the atomic linkages present in the structure. In melanterite, the apical H_2O molecules (Ow6) of the *M*2 octahedra are the only two H_2O molecules, within a M^{2+} coordination sphere, to receive additional H-bonds from neighboring H atoms. The Fe2–Ow6 bond lengthens to 2.169(10) Å to compensate for the reduced bond-valence due to this additional H-bond interaction.

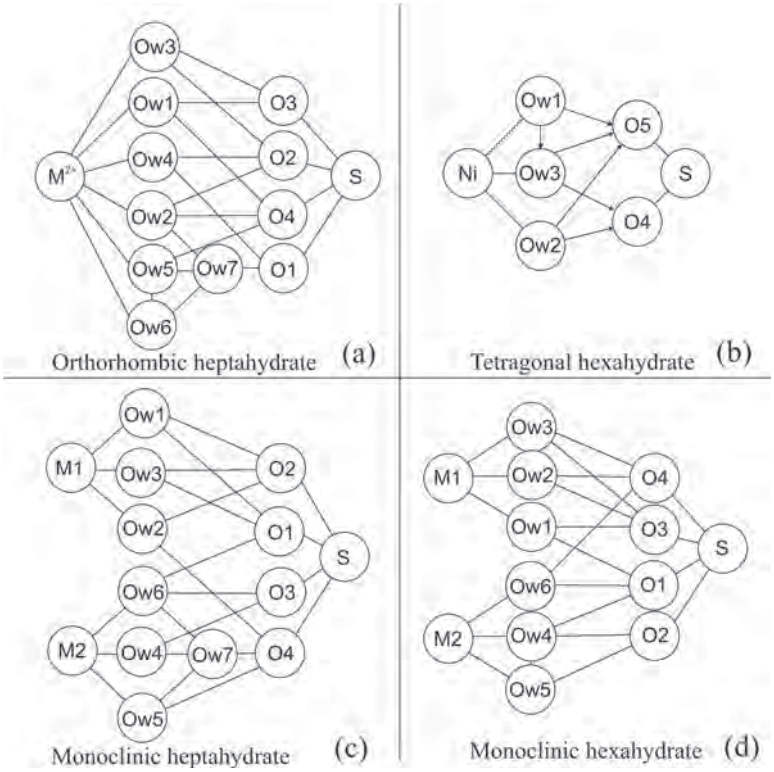

FIG. 7. Hydrogen bonding schemes for (a) orthorhombic heptahydrate structures of the epsomite group, (b) retgersite, a tetragonal hexahydrate, (c) monoclinic heptahydrate structures of the melanterite group, and (d) monoclinic hexahydrate minerals of the hexahydrite group. These diagrams show the distinction between the M^{2+} ions in octahedral coordination with six H_2O molecules that receive two H bonds from external H_2O molecules and those that receive three. Minerals of the general formula $M^{2+}SO_4 \bullet nH_2O$, where n = 5, 4, 3, 1, contain octahedra formed by less than six H_2O molecules and were not considered in this discussion.

more metal substitution than other sulfates is due to the presence of two distinct metal sites and details of the network of H-bonds between metal sites and adjacent polyhedra. The pseudo-face-sharing arrangement of H-bonds between the *M*1 and SO_4 polyhedra and the H-bond interactions between the SO_4 and *M*2 polyhedra, in melanterite, create flexibility of the structure. The melanterite structure is more amenable to incorporation of different metals, and each site may distort differently to accommodate different amounts of metal substitution. In hydrated sulfate minerals, the polyhedra within the structure are held together by a network of H-bonds. Depending on the details of this linkage, this network can provide the structure with both rigidity and flexibility.

ACKNOWLEDGEMENTS

We thank Alison Murray of the Program for Art Conservation, Department of Art at Queen's University for use of the Nicolet ATR–IR spectrometer. The research staff at Chalk River Laboratories (NPMR) provided generous support and materials for this project. We thank George Lager, an anonymous referee and Bob Martin for their helpful comments on this manuscript. An NSERC discovery grant to RCP funded the research.

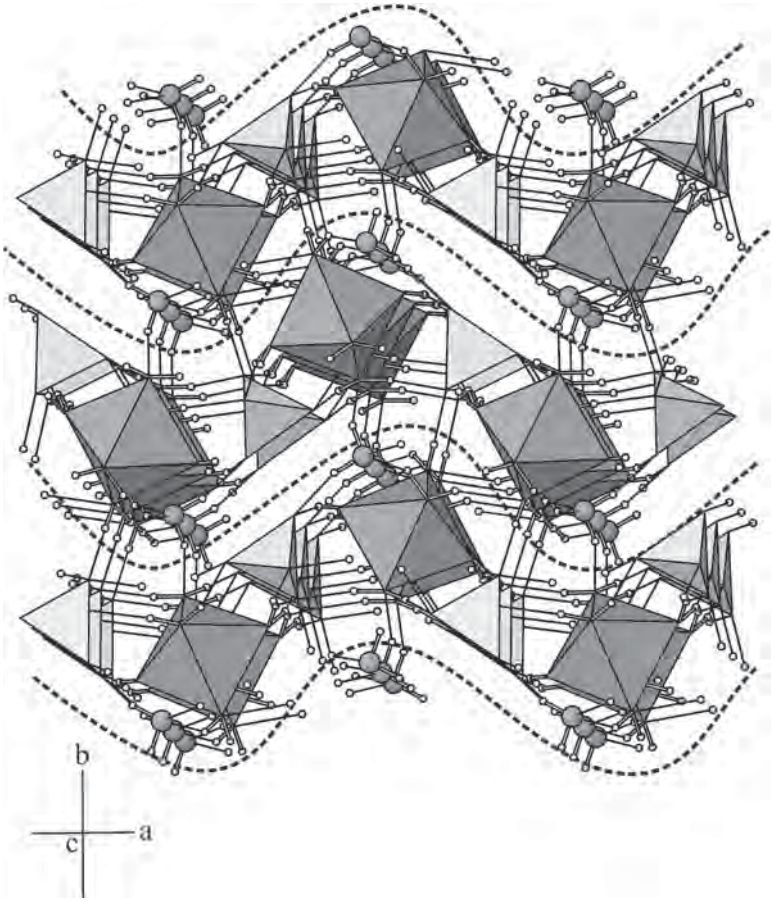

FIG. 8. Schematic representation of the (010) perfect cleavage in epsomite (ATOMS 6.0, Dowty 1995). The cleavage plane is indicated by a solid black undulating line. The H-bonds associated with the interstitial H_2O molecule bridge the layers of octahedra linked to sulfate tetrahedra. This layer in epsomite has a tighter, more corrugated topology than the similar layer of the melanterite structure.

REFERENCES

ANDERSON, J.L. & PETERSON, R.C. (2005): Determination of sulfate mineral phase equilibria as a function of relative humidity. Intermediate compositions in the (Mg,Fe,Zn)SO_4 – H_2O system at 22°C. *Geol. Assoc. Can. – Mineral. Assoc. Can., Program Abstr.* **30**, 4.

ANDERSON, J.L., PETERSON, R.C. & SWAINSON, I.P. (2002): Hydrogen bonding in melanterite. *Int. Mineral. Assoc., 18th Gen. Meeting* (*Edinburgh*), *Abstr.*, 188.

ANDERSON, J.L., PETERSON, R.C. & SWAINSON, I.P. (2005): Combined neutron powder and X-ray single crystal diffraction refinement of the atomic structure and hydrogen bonding of goslarite ($ZnSO_4$•$7H_2O$). *Mineral. Mag.* **69**, 257-269.

ANGEL, R.J. & FINGER, L.W. (1988): Polymorphism of nickel sulfate hexahydrate. *Acta Crystallogr.* **C44**, 1869-1873.

BACON, G.E. & TITTERTON, D.H. (1975): Neutron diffraction studies of $CuSO_4$•$5H_2O$ and $CuSO_4$•$5D_2O$. *Z. Kristallogr.* **141**, 330-341.

BALAREW, V.C. & KARAIVANOVA, V. (1976): Isodimorphe Cokristallisation in Sulfatsystemen als Moglichkeit sur Voraussage der Existenz von Kristallhydraten des Typs MSO_4•nH_2O (M = Mn^{2+}, Fe^{2+}, Co^{2+}, Ni^{2+}, Cu^{2+}, Zn^{2+}, Cd^{2+}). *Z. Anorg. Allg. Chem.* **422**, 283-288.

BARGOUTH, M.O. & WILL, G. (1981): A neutron diffraction refinement of the crystal structure of tetragonal nickel sulfate hexahydrate. *Int. Centre for Theoretical Physics: Rep., Trieste, Italy.*

BAUR, W.H. (1962): Zur Kristallchemie der Salzhydrate. Die Kristallstukturen von $MgSO_4$•$4H_2O$ (Leonhardtit) und $FeSO_4$•$4H_2O$ (Rozenit). *Acta Crystallogr.* **15**, 815-826.

BAUR, W.H. (1964a): On the crystal chemistry of salt hydrates. II. A neutron diffraction study of $MgSO_4$•$4H_2O$. *Acta Crystallogr*. **17**, 863-869.

BAUR, W.H. (1964b): On the crystal chemistry of salt hydrates. IV. The refinement of the crystal structure of $MgSO_4$•$7H_2O$ (epsomite). *Acta Crystallogr.* **17**, 1361-1369.

BAUR, W.H. (1967): On the crystal chemistry of salt hydrates. III. The determination of the crystal structure of $FeSO_4$•$7H_2O$ (melanterite). *Acta Crystallogr*. **17**, 1167-1174.

BAUR, W.H. & ROLIN, J.L. (1972): Salt hydrates. IX. The comparison of the crystal structure of magnesium sulfate pentahydrate with copper sulfate pentahydrate and magnesium chromate pentahydrate. *Acta Crystallogr*. **B24**, 1448-1455.

BLAKE, A.J., COOKE, P.A., HUBBERSTEY, P. & SAMPSON, C.L. (2001): Zinc(II) sulfate tetrahydrate. *Acta Crystallogr*. **E57**, 109-111.

CALLERI, M., GAVETTI, A., IVALDI, G. & RUBBO, M. (1984): Synthetic epsomite, $MgSO_4$•$7H_2O$: absolute configuration and surface features of the complementary (111) forms. *Acta Crystallogr*. **B39**, 218-222.

CHOU, I-MING & SEAL, R.R., II (2003a): Acquisition and evaluation of thermodynamic data for morenosite–retgersite equilibria at 0.1 MPa. *Am. Mineral*. **88**, 1943-1948.

CHOU, I-MING & SEAL, R.R., II (2003b): Determination of epsomite–hexahydrite equilibria by the humidity-buffer technique at 0.1 MPa with implications for phase equilibria in the system $MgSO_4$–H_2O. *Astrobiology* **3**, 619-630.

CHOU, I-MING & SEAL, R.R., II (2005a): Acquisition and evaluation of thermodynamic data for bieberite–moorhouseite equilibria at 0.1 MPa. *Am. Mineral*. **90**, 912-917.

CHOU, I-MING & SEAL, R.R., II (2005b): Determination of goslarite–bianchite equilibria by the humidity-buffer technique at 0.1 MPa. *Chem. Geol*. **215**, 517-523.

CHOU, I-MING, SEAL, R.R., II & HEMMINGWAY B.S. (2002): Determination of melanterite–rozenite and chalcanthite–bonattite equilibria by humidity measurements at 0.1 MPa. *Am. Mineral*. **87**, 108-114.

DOWTY, E. (1995): ATOMS version 6.0. Shape Software, 521 hidden Valley Road, Kingsport, Tennessee 37663, U.S.A. http://www.shapesoftware.com/

ELERMAN, Y. (1988): Refinement of the crystal structure of $CoSO_4$•$6H_2O$. *Acta Crystallogr*. **C39**, 599-601.

ELISEEV, E.N. & SMIRNOVA, S.I. (1958): Iron and magnesium-containing retgersite. *Zap. Vser. Mineral., Obshchest*. **87**, 3-13 (in Russ.).

FERRARIS, G. & FRANCHINI-ANGELA, M. (1972): Survey of the geometry and environment of water molecules in crystalline hydrates studied by neutron diffraction. *Acta Crystallogr.* **B28**, 3572-3583.

FRAU, F. (2000): The formation – dissolution – precipitation cycle of melanterite at the abandoned pyrite mine of Genna Luas in Sardinia, Italy: environmental implications. *Mineral. Mag*. **64**, 995-1006.

FRONCZEK, F.R., COLLINS, S.N. & CHAN, J.Y. (2001): Refinement of ferrous sulfate heptahydrate (melanterite) with low-temperature CCD data. *Acta Crystallogr.* **E57**, 26-27.

GERKIN, R.E. & REPPART, W.J. (1988): Structure of monoclinic nickel(II) sulfate hexahydrate. *Acta Crystallogr*. **C44**, 1486-1488.

GREENSPAN, L. (1977): Humidity fixed points of binary saturated aqueous solutions. *J. Res. Nat. Bur. Stand., A Phys. Chem*. **B1A**, 89-96.

HAWTHORNE, F.C., GROAT, L.A., RAUDSEPP, M. & ERCIT, T.S. (1987): Kieserite, $Mg(SO_4)(H_2O)$, a titanite group mineral. *Neues Jahrb. Mineral., Abh*. **157**, 121-132.

HAWTHORNE, F.C., KRIVOVICHEV, S.V. & BURNS P.C. (2000): The crystal chemistry of sulfate minerals. *In* Sulfate Minerals – Crystallography, Geochemistry and Environmental Significance (C.N. Alpers, J.L. Jambor & D.K. Nordstrom, eds.). *Rev. Mineral. Geochem*. **40**, 1-112.

HEIDE, K. (1965)**:** Weathering of kieserite. *Chem. Erde* **26**, 133-139.

HELD, P. & BOHATY, L. (2002): Manganese(II) sulfate tetrahydrate (ilesite). *Acta Crystallogr.* **E58**, 121-123.

ISKHAKOVA, L.D., DUBROVINSKII, L.S. & CHARUSHNIKOVA, I.A. (1991): Crystal structure, calculation of parameters of atomic interaction potential and thermochemical properties of $NiSO_4$•nH_2O (n = 7,6). *Z. Kristallogr.* **36**, 650-655.

JAMBOR, J.L. (1961): Second occurrence of bonattite. *Can. Mineral*. **7**, 245-252.

JAMBOR, J.L. (1994): Mineralogy of sulfide-rich tailings and their oxidation products. *In* Environmental Geochemistry of Sulfide Mine-Wastes (J.L. Jambor & D.W. Blowes, eds.). *Mineral. Assoc. Can., Short Course Handbook* **22**, 59-102.

JAMBOR, J.L. & BOYLE, R.W. (1964): Moorhouseite and aplowite, new cobalt minerals from Walton, Nova Scotia. *Can. Mineral*. **8**, 166-171.

JAMBOR, J.L. & TRAILL, R.J. (1963): On rozenite and siderotil. *Can. Mineral*. **7**, 751-763.

KELLERSOHN, T. (1992): Structure of cobalt sulfate tetrahydrate. *Acta Crystallogr.* **C48**, 776-779.

KELLERSOHN, T., DELAPLANE, R.G. & OLOVSSON, I. (1991): Disorder of a trigonally planar coordinated water molecule

in cobalt sulfate heptahydrate, $CoSO_4•7D_2O$ (bieberite). *Z. Naturforsch*. **46**, 1635-1640.

Larson, A.C. & Von Dreele, R.B. (2000): General Structure Analysis System (GSAS). Los Alamos National Laboratory, Rep. **LAUR 86-748.**

Leverett, P., McKinnon, A.R. & Williams, P.A. (2004): New data for boothite, $CuSO_4•7H_2O$, from Burraga, New South Wales. *Aust. J. Mineral*. **10**, 3-6.

Oleinikov, B.V., Shvartsev, S.L., Mandrikova, N.T. & Oleinikova, N.N. (1965): Nickelhexahydrate, a new mineral. *Zap. Vser. Mineral., Obshchest*. **94**, 534-547.

Pannetier, G., Bregeault, J.M & Tardy, M. (1965): Etude de la dissociation thermique des sulfates et des sulfates basiques. VI. Mise en evidence et étude cristallographique du sulfate de zinc tétrahydraté $ZnSO_4•4H_2O$. *Mémoires Présentés à la Société Chimique* **55**, 324-326.

Pašava, J., Breiter, K., Huka, M. & Korecký, J. (1986): Chvaleticeite, $(Mn,Mg)SO_4•6H_2O$, a new mineral. *Neues Jahrb. Mineral., Monatsh*., 121-125.

Peterson, R.C. (2003a): The relationship between Cu content and distortion in the atomic structure of melanterite from the Richmond mine, Iron Mountain, California. *Can. Mineral*. **41**, 937-949.

Peterson, R.C. (2003b): Dehydration of minerals in mine waste. The relationship among melanterite $FeSO_4•7H_2O$, siderotil $FeSO_4•5H_2O$, and rozenite $FeSO_4•4H_2O$. *Geol. Assoc. Can. – Mineral. Assoc. Can., Program Abstr.* **28**, SS4.

Peterson, R.C. & Grant, A. (2005): Dehydration and crystallization reactions of secondary sulfate minerals found in mine waste: *in situ* powder-diffraction experiments. *Can. Mineral*. **43**, 1171-1181.

Peterson, R.C., Hammarstrom, J.M. & Seal, R.R., II (2006): Alpersite $(Mg,Cu)SO_4•7H_2O$ a new mineral of the melanterite group, and cuprian pentahydrite: their occurrence within mine waste. *Am. Mineral*. **19**, 261-269.

Ptasiewicz-Bak, H., Olovsson, I. & McIntyre, G.J. (1993): Bonding deformation and superposition in the electron density of tetragonal $NiSO_4•6H_2O$ at 25 K. *Acta Crystallogr*. **B49**, 192-201.

Sinha, S.G. & Deshpande, N.D. (1989): Thermal dehydration of crystalline $NiSO_4•6H_2O$. *Thermochimica Acta* **144**, 83.

Sinha, S.G., Deshpande, N.D. & Deshpande D.A. (1989): Dehydration of crystalline $CoSO_4•7H_2O$. *Thermochimica Acta* **156**, 1-10.

Srebrodol'skii, B.I. (1977a): Products of epsomite dehydration. *Konstitutsiya i Svoistva Mineralov* **11**, 103-105 (in Russ.).

Srebrodol'skii, B.I. (1977b): Products of melanterite alteration. *Dopovidi Akad. Nauk Ukrains'koi RSR, Seriya B: Geologichni, Khimichni ta Biologichni Nauki* **9**, 797-800 (in Russ.).

Strens, R.G.J. (1966): The axial-ratio-inversion effect in Jahn–Teller distorted ML_6 octahedra in the epidote and perovskite structures. *Mineral. Mag*. **35**, 777-781.

Walenta, K. (1978): Boyleit, ein neues Sulfatmineral von Kropback im südlichen Schwarzwald. *Chem. Erde* **37**, 73-79.

Wildner, M. & Giester, G. (1991): The crystal structures of kieserite-type compounds. I. Crystal structures of $Me(II)SO_4\ H_2O$ (Me= Mn, Fe, Co, Ni, Zn). *Neues Jahrb. Mineral., Monatsh.,* 296-306.

Zahrobsky, R.F. & Baur, W.H. (1968): On the crystal chemistry of salt hydrates. V. The determination of the crystal structure of $CuSO_4•3H_2O$ (bonattite). *Acta Crystallogr*. **B24**, 508-513.

Zalkin, A., Ruben, H. & Templeton, D.H. (1967): The crystal structure and hydrogen bonding of magnesium sulfate hexahydrate. *Acta Crystallogr*. **17**, 235-240.

Received April 14, 2006, revised manuscript accepted November 9, 2006.